Numerical Investigation of Heat Transfer Characteristics of Ribs with Trenches in Gas Turbine Internal Cooling Channel

Tuong-Linh Nha, Khanh-Duy Cong Do, Van-Thuc Tran, Viet-Dung Duong, Sung-Goon Park, and Cong-Truong Dinh

Abstract In this work, several trenches are placed in the ribs to reduce disadvantages of square ribs. These configurations open up some small extra passages for the coolant to remove the local vortices. Furthermore, the remained square pillars of the ribs act like pin-fins which promote horseshoe vortices. These vortices significantly enhance the heat transfer capability in the junction of pillars and endwall. To investigate the effect of trenches number and shape on the heat transfer capacity of the channel and flow characteristics, a parametric study of ribs with trenches is performed using RANS equations with the SST turbulence model. Furthermore, the staggered and in-line arrangements of ditches are studied. It is concluded that the staggered trenches show a higher Nusselt number than the in-line arrangement, but it comes with a higher friction factor. The parametric study resulted in a higher heat transfer efficiency index (HTEI) of the new designs than the square ribs. At Re = 26,500, the Nusselt number of 3 trenches with staggered arrangement increases by 41.9%. Moreover, a slight increase in friction factor combines with that to form a 31.9% increase in the overall Heat transfer efficiency index. The designs of 3 trenches with in-line arrangement come with a slight increase of 13.7% in Nusselt number; a decrease in friction factor of this design forms a 16.4% increase in Heat transfer efficiency index compared to the case of the original ribs.

T.-L. Nha (✉) · K.-D. C. Do · V.-T. Tran · C.-T. Dinh
Ha Noi University of Science and Technology, No. 1, Dai Co Viet Road, Hai Ba Trung District, Hanoi 10000, Vietnam
e-mail: linh.nhatuong@hust.edu.vn

V.-D. Duong
School of Aerospace Engineering, Vietnam National Univerisity, University of Engineering and Technology, Hanoi City, Vietnam

S.-G. Park
Department of Mechanical Engineering and Automotive Engineering, Seoul National University of Science and Technology, No 232 Gongreung-Ro, Nowon-Gu, Seoul, Korea

B. T. Long et al. (eds.), *Proceedings of the 3rd Annual International Conference on Material, Machines and Methods for Sustainable Development (MMMS2022)*, Lecture Notes in Mechanical Engineering,
https://doi.org/10.1007/978-3-031-31824-5_13

Keywords Heat transfer characteristics · Ribs with trenches · RANS analysis · Internal cooling

1 Introduction

By avoiding the blending of cooling air and hot gas coming from the combustor, the internal cooling method, which includes three main forms, i.e., impinging jet cooling, rib turbulators cooling [1], and pin-fins cooling, provides a more reliable turbine's aerodynamic performance. The rib turbulators, which can enhance local turbulence due to flow separation and confluence in turbine blade serpentine channels, are the subject of research in this paper. Pham et al. [2] studied the influence of rib profiles on the HTEI and the obtained results showed that the HTEI changed significantly when changing the rib profiles. Another study by Dinh et al. [3] investigated a clearance height of 20% compared to the height of the ribs yields the highest HTEI. For cooling channel, the different cooling gases produce different heat transfer characteristics. Shi et al. [4] studied experimentally the differences between steam and air used in a cooling channel with different angled ribs. They found that when steam is used as a coolant of gas turbine internal cooling passage, heat transfer is enhanced significantly.

Besides ribs, pin–fin is another type of structure that promotes turbulence in the cooling cascade of the channel. Do et al. [5] studied the effect of endwall on enlarging the size of high heat transfer region and reducing the low heat transfer regions in channel with pin-fins. Won et al. [6] studied the distribution of heat transfer coefficient in a cooling channel with multiple rows of pin-fins. Based on the results of Shi et al. [4] of the channel with 90º ribs, this work investigated the effects of trenches on the heat transfer characteristics of channels.

2 Numerical Methodology

2.1 Description of Geometry

The computational domain was constructed based on the experimental model of Shi et al. [4] as shown in Fig. 1. The testing sample of Shi et al. [4] consists of three channels: the development, the heated, and the output, where 12 ribs are attached to the heated channel. The height and sample width of the tested channel are W = 80 mm and H_s = 20 mm, respectively, and the top surface of the channel is specified as symmetry to simplify the channel. Hence, the real height of the total channel is H = 40 mm. The cross-section of the computed domain is a rectangle with the aspect ratio AR = W/H = 80/40 = 2. The equivalent diameter of the channel, $D_h = 2HW/(H + W)$ is 53.3 mm. The direction of the flow corresponds to the direction of the x-axis. The detailed dimensions of the design model are given in Table 1. The total length

of the calculated domain is $L_t = 600$ mm. Table 1 describes the design variables of the tested channel.

The number of trenches varies from three to five with in-line and staggered arrangements. The trenches were distributed evenly on the y-direction of ribs in the channel, spread from the middle of the channel for the opposition. The number of trenches will vary from 3 to 5 trenches a rib. Figure 2 illustrates specifically the overview of ribs with trenches of in-line and staggered arrangements.

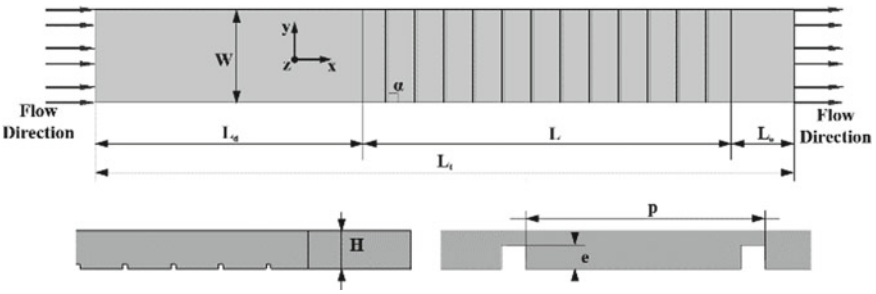

Fig. 1 Schematic diagram of geometric configurations

Table 1 Variables of geometric configurations

Variable	Value	Variable	Value
W (mm) × H_s (mm)	80 × 20	α	90°
e (mm)	2.5	L_d (mm)	230
p (mm)	25	L (mm)	316
D_h (mm)	53.33	L_o (mm)	54

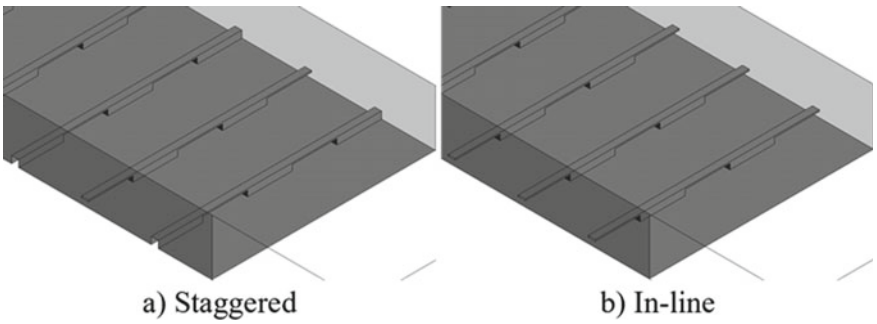

Fig. 2 Sample of design arrangements for trenches

2.2 Data Reduction

The Reynolds number (Re) of the channel is defined as:

$$Re = \frac{\rho u D_h}{\mu} \tag{1}$$

where u is the inlet velocity of the channel; ρ is the air density, D_h and μ are the channel hydraulic diameter and dynamic viscosity of the coolant, respectively.

The local heat transfer coefficient (h) of the heated surfaces is determined by:

$$h = \frac{q}{T_w - T_b} \tag{2}$$

where q is the heat flux of the heated wall, T_w is wall temperature, and T_b is the bulk temperature of the fluid.

The local Nusselt number (Nu) is used to represent the local heat transfer capacity, which can be written as:

$$Nu = \frac{h D_h}{\lambda} \tag{3}$$

where λ is the thermal conductivity of coolant fluid.

According to the correlation formula of Dittus-Boelter [7], the Nusselt number (Nu_0) and friction factor for fully developed turbulent flow in a smooth channel of a rectangular cross-section is defined as:

$$Nu_0 = 0.023.Re^{0.8} Pr^{0.4} \tag{4}$$

$$f_0 = [1.58 \ln(\mathrm{Re}) - 3.28]^{-2} \tag{5}$$

The friction factor which represents the pressure loss of the channel is defined as:

$$f = \frac{\Delta P D_h}{2\rho \Delta L u^2} \tag{6}$$

The heat transfer efficiency index (η) is defined as:

$$\eta = \left(\frac{Nu}{Nu_0}\right) / \left(\frac{f}{f_o}\right)^{1/3} \tag{7}$$

2.3 Numerical Analysis

In the present study, the governing differential equations are solved numerically to study the flow characteristics and heat transfer in the channel with pin-fins using the commercial software Ansys CFX® 19.1 [8]. The SST turbulence model is used for all the simulations throughout the work. This work uses the structured grid divided in ANSYS-ICEM® software. The elements adjacent to the wall and the pin-fins are specified with a height of 5×10^{-6} (m) to satisfy a y^+ value less than 1 for the entire Reynolds number range, to fit the criteria of the turbulence model. The structural grid shown in Fig. 3 is created using hexahedral elements. The test grid will be used for Reynolds 53,648, and the number of grids will vary from 1.0 million to 11.5 million.

The boundary conditions adopted here are used the same as the Ref. [4] as shown in Fig. 4. The fluid was set as steam (IAPWS-97). The walls both in the entrance and in the outlet section are specified as adiabatic. A uniform heat flux of 5000 W/m^2 is allocated at the ribbed surfaces and the two sides of smooth walls. The reference pressure of the computational domain and the inlet temperature of steam flow was 0.3 MPa and 447 K, respectively. The outlet was subject to static pressure of 0 Pa. The mass flow rate was given at the inlet according to the corresponding Reynolds numbers ranging from 9098 to 53,648. A turbulence intensity of 5% was given at the inlet. The walls of the channels were applied as the no-slip boundary condition.

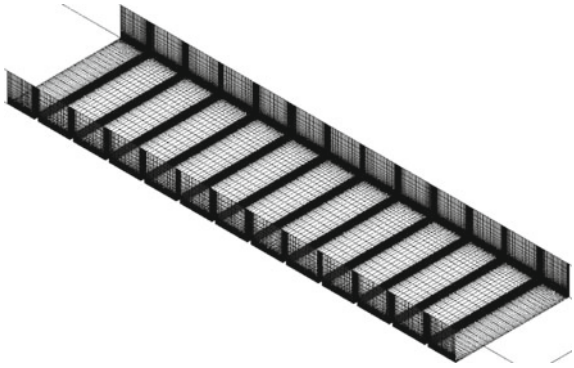

Fig. 3 Sample of mesh structure

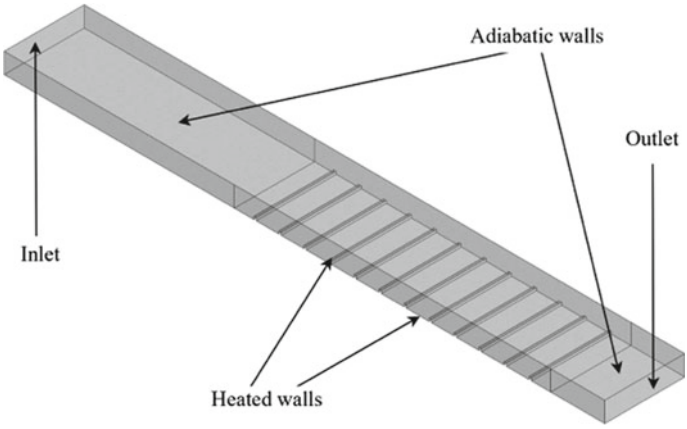

Fig. 4 Boundary conditions

3 Results and Discussion

3.1 Grid Independence Test and Validation of Numerical Results

A grid independence test has been conducted by using the SST k-ω model at Re = 53,648 with mesh numbers ranging from 1 to 11.5 million. The grid convergence index (GCI) based on the Richardson extrapolation method was analyzed to evaluate the convergence of the grid system used in this study. Table 2 lists the results of the GCI analysis for the channel with ribs. In Fig. 5, the Nusselt number increase when decreasing the normalized grid spacing. It is shown that the Nusselt number is converging to the value of extrapolation by Richardson's method. Grid 2 was selected for further computation.

In order to validate the SST k-ω model, a comparison of numerical and experimental results of averaged Nusselt number distribution on the heated walls for three Reynolds numbers (9098, 26,587, 53,648) is shown in Fig. 6, where the boundary conditions are also in accordance with the experimental investigations [4]. The averaged Nu numbers on the heated walls for Re = 9098, 26,587, and 53,648 are 0.03%, 3.09%, and 8.09% higher than that of experimental data. This is partly because the uncertainty of 8.5% exists in the experimental system. Therefore, the numerical deviations are acceptable.

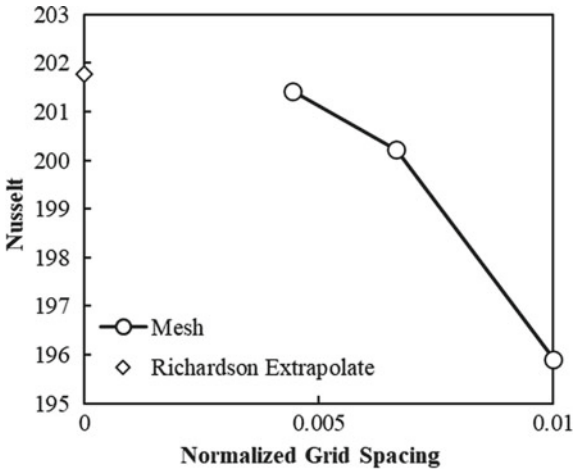

Fig. 5 Comparison of investigated mesh with Richardson extrapolation

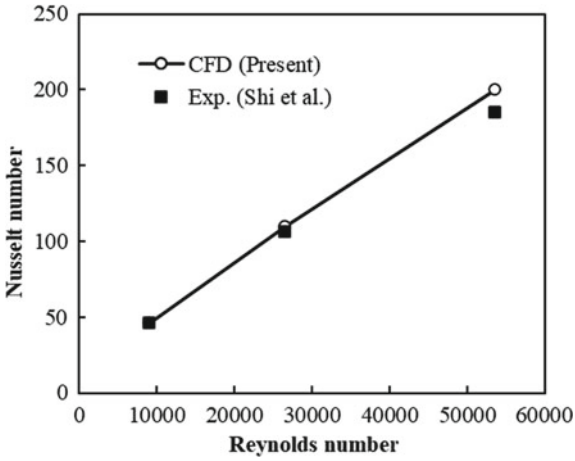

Fig. 6 Comparison of experimental and numerical data with Re = 53,648

Table 2 Results of analysis of grid convergence

Parameter	Symbol	Value
Numbers of elements (milliin cells)	Grid 1/Grid 2/Grid 3	11.5/3.4/1.0
Grid refinements factors	r_{21}/r_{32}	1.50/1.50
Normalized grid spacing	$h_1/h_2/h_3$	0.0100/0.0067/0.0044
Nusselt number corresponding to Grid 1/Grid 2/Grid 3	$Nu_1/Nu_2/Nu_3$	201.429/200.223/195.912
Apparent order	p	3.12
Extrapolated value	ϕ_{ext}^{21}	201.9023
Approximated relative error	e_a^{21}	0.60%
Extrapolated relative error	e_{ext}^{21}	0.23
Grid convergence index	GCI_{fine}^{21}	0.29

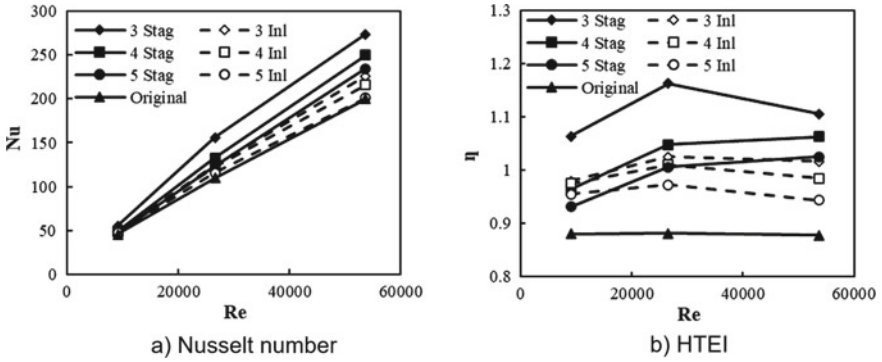

Fig. 8 Comparisons of Nu and η with all cases

3.2 Effect of Ribs with Trenches on Convective Heat Transfer

Figure 8 shows the comparison of Nu, and η with the cases of 3, 4, and 5 trenches with both arrangements. It is discovered that the staggered arrangements induce a higher Nusselt number for all cases compared to the in-line arrangements but accompany by a higher friction factor. The Nusselt number is increased by about 20.1%, 41.9%, and 36.5% for three Re of 9098, 26,587, and 53,648 for the case of 3 trenches with the staggered arrangement and it is increased by 7.9%, 13.7%, and 12.9% for in-line arrangement. Overall, the HTEI of staggered designs is increased by 20.8%, 31.9%, and 26.0% and that of in-line designs show an increase by 11.3%, 16.4%, and 15.8% for all Reynolds number.

4 Conclusion

The results show that the trenches open up some extra passages for the flow to destruct the stagnant vortices in front of and behind the ribs and increase the heat transfer characteristics in the heated walls and the ribs. Besides, the staggered arrangement induces a higher Nusselt number than the in-line cases and hence, creates a higher friction factor. However, the increase in Nusselt number is higher than the increase in friction factor and the overall HTEI is increased. The HTEI of staggered designs is increased by 20.8%, 31.9%, and 26.0% compared to the original design for Re = 9098, 26,587, and 53,648, respectively. Besides, the in-line arrangement comes with a maximum increase of 13.7% in the Nusselt number for Re = 26,587. It combines with a decrease of 9.3% in friction factor to form an increase of 16.4% in HTEI.

Acknowledgements This study is funded by Hanoi University of Science and Technology (HUST) under grant number T2022-PC-018.

References

1. Moon MA, Kim KY (2016) Exergetic analysis for optimization of a rotating equilateral triangular cooling channel with staggered square ribs. Int J Fluid Mach Syst 9(03):229–236. https://doi.org/10.5293/IJFMS.2016.9.3.229
2. Pham KQ, Nguyen QH, Vu TD, Dinh CT (2020) Effects of boot-shaped rib on heat transfer characteristics of internal cooling turbine blades. J Heat Transf 142(10):102106. https://doi.org/10.1115/1.4047490
3. Dinh CT, Nguyen TM, Vu TD, Park SG, Nguyen QH (2021) Numerical investigation of truncated-root rib on heat transfer performance of internal cooling turbine blades. Phys Fluids 33(7). https://doi.org/10.1063/5.0054149
4. Shi X, Gao J, Xu L, Li F (2013) Heat transfer efficiency index comparison of steam and air in gas turbine cooling channels with different rib angles. Heat Mass Transf 49(11):1577–1586. https://doi.org/10.1007/s00231-013-1171-6
5. Do KD, Chung DH, Tran DQ, Dinh CT, Nguyen QH, Kim KY (2022) Numerical investigation of heat transfer characteristics of pin-fins with roughed endwalls in gas turbine blade internal cooling channels. Int J Heat Mass Transfer 195:123125. https://doi.org/10.1016/j.ijheatmasstransfer.2022.123.125
6. Won SY, Mahmood GI, Ligrani PM (2004) Spatially-resolved heat transfer and flow structure in a rectangular channel with pin fins. Int J Heat Mass Transf 47(8–9):1731–1743. https://doi.org/10.1016/j.ijheatmasstransfer.2003.10.007
7. Dittus FW, Boelter LMK (1985) Heat transfer in automobile radiators of the tubular type. Int Commun Heat Mass Transfer 12(1):3–22. https://doi.org/10.1016/0735-1933(85)90003-x
8. ANSYS CFX 19.1 (2018) ANSYS CFX-solver theory guide, ANSYS Inc